DALTON

Redox regulation in ruthenium(II) polypyridyl complexes and their application in solar energy conversion

Mohammad K. Nazeeruddin,*,† Edgar Müller, Robin Humphry-Baker, Nick Vlachopoulos and Michael Grätzel *

Laboratory for Photonics and Interfaces, Institute of Physical Chemistry, Swiss Federal Institute of Technology, CH-1015 Lausanne, Switzerland

Ruthenium(II) complexes of the type [Ru(dmbip)(Hdcbpy)X], [Ru(dmbip)(Hdcbiq)X] and [Ru(dhbip)(Hdcbpy)X], where dmbip = 2,6-bis(1-methylbenzimidazol-2-yl)pyridine, dhbip = 2,6-bis(1-hexadecylbenzimidazol-2-yl)pyridine, H_2dcbpy = 4,4′-dicarboxy-2,2′-bipyridine, H_2dcbiq = 4,4′-dicarboxy-2,2′-biquinoline and X = Cl^-, NCS^-, CN^- or H_2O, have been synthesized and spectroscopically characterized. They act as efficient charge-transfer sensitizers, when anchored onto nanocrystalline TiO_2 films. The lowest-energy metal-to-ligand charge-transfer transitions in these complexes could be tuned from 500 to 590 nm by choice of appropriate ligands and the highest occupied molecular orbital varied over 400 mV. Some of the complexes reported are emissive at room temperature. The ground- and excited-state pK_a values of dcbpy complexes were measured by spectrophotometric and spectrofluorimetric titration. Resonance-Raman spectra show bands characteristic of the dmbip and dcbpy ligand for excitation at 468 nm, while excitation at 568 nm gave predominantly bands associated with the dcbpy ligand. The excited-state pK_a values and the resonance-Raman data indicate that the lowest excited state is a metal to dcbpy or dcbiq ligand charge-transfer state.

The photophysical and photochemical properties of Group VIII metal complexes using terpyridine (terpy) and bipyridine ligands have been thoroughly investigated during the last two decades.[1–5] The main thrust behind these studies is to understand the energy- and electron-transfer processes in the excited state and to apply this knowledge to potential practical applications like solar energy conversion and light-driven information processing.[6] Ruthenium(II) complexes containing 4,4′-dicarboxy-2,2′-bipyridine ligand (H_2dcbpy) have been used extensively during the last 10 years[7] as charge-transfer sensitizers on nanocrystalline TiO_2 films in our laboratory. The photoexcitation of the metal-to-ligand charge transfer (MLCT) of the adsorbed dye leads to injection of electrons into the conduction band. The efficiency of this electron-transfer process has been reported to be 95% for monochromatic light.[8]

The key requirements for an efficient sensitizer are: (*i*) the excited state should have enough thermodynamic driving force for the injection of electrons into the conduction band, (*ii*) the oxidized sensitizer should be stable, in order to be quantitatively reduced back by an electron donor or an electron-relay system and (*iii*) the dye MLCT absorption should overlap with the solar emission spectrum in order to get maximum power conversion. In this paper we discuss ways to tune the MLCT absorption to get an optimum spectral overlap with the solar emission.

The MLCT transitions of the polypyridyl complexes of ruthenium can be tuned in two ways. First, by introducing a ligand with a low-lying π* molecular orbital such as 2,2′-biquinoline and 2,3-dipyridylpyrazine.[9] In ruthenium(II) complexes containing such ligands the MLCT transitions are considerably red shifted. Secondly by destabilization of the metal t_{2g} orbital with a strong donor ligand. With suitable ligands it is possible to shift the metal-centered oxidation potential in such complexes over a range of 1 V.[10] For an efficient sensitizer these two extreme conditions are not compatible, because in the former case, the excited state is not sufficiently energetic to enable electron transfer into the conduction band of the TiO_2 semiconductor, and in the latter case the easily oxidizable complex cannot be reduced back by a suitable electron relay.

Recently, using the above mentioned concepts (ligands having low π* orbital and strong σ-donor capacity), Meyer and co-workers[11] have tuned the MLCT transitions from *ca*. 450 to *ca*. 568 nm in ruthenium complexes containing three different bidentate ligands. However, there are only a few reports on MLCT and redox tuning of terpyridine and substituted terpyridine complexes of ruthenium.[12] The main reasons for such a limited study on terpyridine complexes are the lack of synthetic routes for substituted terpyridines and the short excited-state lifetime of these complexes.[13]

We report here the synthesis of a new family of ruthenium complexes with a planar tridentate ligand such as 2,6-bis-(1-methylbenzimidazol-2-yl)pyridine (dmbip), where the methyl group can be substituted by an electron-donor or -acceptor functionality.[14] The other co-ordination sites are occupied by dcbpy or 4,4′-dicarboxy-2,2′-biquinoline (H_2dcbiq) ligands and a pseudo-halide anion. Unlike the terpyridine ligand, dmbip acts as a hybrid ligand having both strong σ-donor (benzimidazole unit) and π-acceptor (pyridine ring) properties. Thus, by an appropriate choice of the substituents on the imidazole nitrogen, it is now possible to tune the ground and excited-state properties in a more predictable manner. The carboxyl groups of the ligand provide the grafting functionalities to the oxide surface, ensuring intimate electronic coupling between the sensitizer and the semiconductor. This type of electronic interaction is required to facilitate rapid electron transfer between the excited state of the sensitizer and the conduction band. The near-unity incident photon-to-current conversion efficiency (IPCE) of these complexes illustrate, the very efficient electronic coupling between the π* orbital of the dcbpy ligand and the 3d orbital of the TiO_2 semiconductor.

Experimental

The UV/VIS spectra were recorded on a Varian Cary 5 or HP 8450A diode-array spectrophotometer, emission spectra with a Spex Fluorolog spectrofluorimeter equipped with a Hamamatsu R2658 photomultiplier tube. All emission spectra

† E-Mail: mdkhaja.nazeeruddin@icp.dc.epfl.ch.

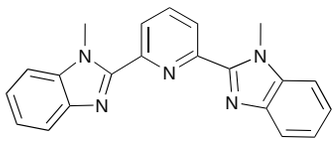

dmbip = 2,6-bis(1-methylbenzimidazol-2-yl)pyridine

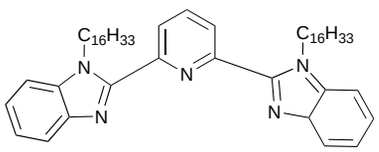

dhbip = 2,6-bis(1-hexadecylbenzimidazol-2-yl)pyridine

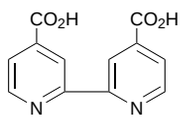

H_2dcbpy = 4,4′-dicarboxy-2,2′-bipyridine

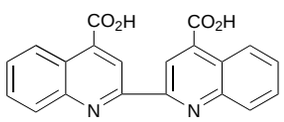

H_2dcbiq = 4,4′-dicarboxy-2,2′-biquinoline

were photometrically corrected. The samples were measured under oxygen-free conditions. Low-temperature measurements were carried out in an Oxford Instruments DN1704 N_2 cryostat. Proton and ^{13}C NMR spectra were recorded on a Bruker AC-P 200 MHz spectrometer, infrared with a Perkin–Elmer Paragon 1000 FTIR spectrophotometer at a resolution of 5 cm^{-1} with the samples in compressed KBr pellets. Cyclic voltammetry measurements were carried out with a PAR 273 A model potentiostat. A two-compartment cell with a three-electrode system, glassy carbon as a working electrode, was used. The solvents used in the electrochemical studies were either freshly distilled or of analytical grade. In all measurements, 0.1 M tetrabutylammonium tetrafluoroborate or triflate (trifluoromethanesulfonate) was used as supporting electrolyte. Solutions were thoroughly purged with argon and during the measurements a positive pressure of argon was kept over the sample.

Resonance-Raman (RR) spectra were obtained on a SPEX Industries 1877 Triplemate Spectrograph equipped with a Princeton Instruments liquid-N_2 cooled CCD-1024E detector. A 1200 groove per mm grating was used giving a resolution of 2.5 cm^{-1}. Data acquisition was controlled by an Apple PowerPC computer running WAVEMETRICS software to control the PI ST-135 controller and the DM3000 controller. All the data were corrected for the spectral response of the instrument using a National Bureau of Standards light standard. A Coherent INNOVA 200K Kr^+ laser provided the excitation source. Aqueous solutions of typically 0.5 mM concentration were measured in 1 mm inner diameter capillaries, using a 90° scattering geometry.

Materials

The compounds 2,6-bis(1-methylbenzimidazol-2-yl)pyridine (dmbip) and 2,6-bis(1-hexadecylbenzimidazol-2-yl)pyridine (dhbip) were synthesized using a reported method;[15] H_2dcbpy, H_2dcbiq and $RuCl_3 \cdot 3H_2O$ were obtained from Fluka and Johnson Matthey, respectively. All the solvents used in the preparative work were obtained commercially and used without further purification.

Synthesis

[Ru(dmbip)Cl_3] 1 and [Ru(dhbip)Cl_3] 2. The method used is similar to that reported by Moyer and Meyer[16a] for terpyridine complexes, and Kohle *et al.*[16b] for dmbip. In a typical synthesis, commercial $RuCl_3 \cdot 3H_2O$ (0.523 g, 2 mmol) was dissolved in ethanol (100 cm^3) under a nitrogen atmosphere. To this solution was added 2,6-bis(1-hexadecylbenzimidazol-2-yl)pyridine (1.519 g, 2 mmol) and the mixture was refluxed for an hour with continuous stirring. After cooling the reaction flask to room temperature, the precipitate was collected on a sintered glass crucible and washed with a generous amount of ethanol followed by diethyl ether. The product was air dried using a water pump. The yield was 1.85 g (96%).

[Ru(dmbip)(H_2dcbpy)Cl]Cl 3, [Ru(dmbip)(H_2dcbiq)Cl]Cl 4 and [Ru(dhbip)(H_2dcbpy)Cl]Cl 5. The synthetic details for complex **5**, as representative, are given. Complex **2** (0.515 g) was taken in a three-necked round-bottom flask (100 cm^3) and dissolved in dimethylformamide (dmf) (30 cm^3) under nitrogen. To this solution H_2dcbpy (0.13 g) was added. After refluxing for 5 h with stirring, the reaction mixture was allowed to cool to room temperature and filtered. The filtrate was evaporated on a rotational evaporator and the resulting solid washed with low-boiling light petroleum (b.p. 30–40 °C), followed by water to remove inorganic salts. The insoluble solid was dissolved in dmf (10 cm^3) and allowed to crystallize by slow diffusion of diethyl ether. The suction-dried product weighed 0.540 g (85%).

[Ru(dmbip)(Hdcbpy)(CN)] 6, [Ru(dmbip)(Hdcbpy)(NCS)] 7, [Ru(dhbip)(Hdcbpy)(NCS)] 8 and [Ru(dmbip)(Hdcbiq)(NCS)] 9. The chloride anion in complexes **3**–**5** was exchanged by refluxing in dmf with a 20-fold excess of a pseudo-halogen salt under nitrogen. In a typical synthesis, KNCS (0.343 g) was taken into a three-necked flask containing dmf (100 cm^3) and [Ru(dhbip)(H_2dcbpy)Cl] **5** was added. The reaction mixture was refluxed for 5 h with stirring then the flask was cooled and the solution was filtered through a sintered-glass crucible. The filtrate was evaporated to dryness on a rotational evaporator. The resulting solid was washed once with acetone, followed by low-boiling light petroleum. Finally the solid was washed with water to remove the excess of free thiocyanate and inorganic salts. The insoluble solid was dissolved in dmf (10 cm^3) and allowed to crystallize by slow diffusion of diethyl ether. After suction drying the yield was 0.1 g (49%).

[Ru(dmbip)(dcbpy)(H_2O)] 10. This complex was obtained by the substitution of chloride by water. In a typical synthesis, the chloro precursor complex **3** (0.5 g) was slowly digested in water (30 cm^3) by the addition of 0.1 M NaOH solution. The base was added to the chloro complex in such a way as to keep the pH below 9, in order to avoid formation of possible higher-oxidation-state ruthenium complexes. After allowing the solution to stand for 3 h at pH 9 with stirring, it was neutralized to pH 4 by the addition of 0.1 M $HClO_4$ solution. At this pH most of the complex precipitates as a neutral salt. Yield 80%. [**CAUTION:** perchlorate salts are highly explosive and extreme care should be taken while handling. One should not scratch or evaporate or heat, in particular in the presence of organic solvents.]

Results and Discussion

Syntheses of all the ruthenium complexes were carried out in an inert atmosphere under reduced light. The complexes were isolated as neutral species as a result of the deprotonation of carboxy groups at around pH 2–3. Ruthenium complexes containing dcbiq ligand required longer refluxing times in dmf than did the bipyridine analogues. All the ruthenium complexes presented gave satisfactory elemental analysis (Table 1).

Table 1 Analytical data for the complexes with calculated values in parentheses

Complex	Analysis (%) C	H	N	Cl
1 $[Ru^{III}(dmbip)Cl_3]\cdot 4H_2O$	46.03 (46.06)	3.15 (3.13)	12.9 (12.79)	19.8 (19.44)
2 $[Ru^{III}(dhbip)Cl_3]\cdot 3H_2O$	60.21 (60.03)	7.75 (8.0)	6.95 (6.86)	11.00 (10.44)
10 $[Ru^{II}(dmbip)(dcbpy)(H_2O)]\cdot 8H_2O$	46.65 (46.89)	4.51 (4.64)	11.73 (11.60)	—
7 $[Ru^{II}(dmbip)(Hdcbpy)(NCS)]\cdot 8H_2O$	45.78 (46.0)	3.78 (4.55)	12.42 (12.64)	
6 $[Ru^{II}(dmbip)(Hdcbpy)(CN)]\cdot 6H_2O$	49.84 (49.98)	4.35 (4.44)	13.64 (13.71)	
$[Ru^{II}(dmbip)(H_2dcbiq)(NCS)]ClO_4\cdot 3H_2O$	52.0 (52.82)	3.69 (3.65)	12.95 (11.61)	—
8 $[Ru^{II}(dhbip)(Hdcbpy)(NCS)]\cdot H_2O$	64.41 (65.39)	7.14 (7.32)	9.75 (9.54)	—

Table 2 Absorption and luminescence properties of the ruthenium complexes in EtOH

Complex	Absorption λ_{max}/nm ($\varepsilon/10^4$ M^{-1})[a] π–π* dmbip or dhbip	π–π* dcbpy or dcbiq	$d_{\pi-\pi^*}$	Emission λ_{max}/ nm at 298 K	τ/ ns at 298 K
1 $[Ru^{III}(dmbip)Cl_3]$	339, 354	—	446	—	—
2 $[Ru^{III}(dhbip)Cl_3]$	340, 356	—	446	—	—
3 $[Ru^{II}(dmbip)(Hdcbpy)Cl]$	344 (2.8), 360 (3.4)	308 (3.8)	516	—	—
10 $[Ru^{II}(dmbip)(dcbpy)(H_2O)]$	344 (2.8), 361 (3.3)	307 (3.9)	508	800	<5
[b]	345 (3.0), 359 (3.7)	314 (4.0)	511 (1.2)		
$[Ru^{II}(dmbip)(Hdcbpy)(OH)]$[c]	343 (2.8), 358 (3.5)	309 (3.76)	528 (1.05)	800	<5
7 $[Ru^{II}(dmbip)(Hdcbpy)(NCS)]$	346 (3.4), 362 (4.1)	307 (4.7)	502 (1.4)	800	34
6 $[Ru^{II}(dmbip)(Hdcbpy)(CN)]$	342 (3.1), 357 (4.2)	306 (4.1)	486 (1.35)	750	130
4 $[Ru^{II}(dmbip)(H_2dcbiq)Cl]Cl$	348 (5.1) —	320 (4.9)	608 (0.89)	—	—
$[Ru^{II}(dmbip)(H_2dcbiq)(NCS)]ClO_4$	348 (5.9), 362 (4.5)	320 (5.0)	580 (0.97)	900	<5
5 $[Ru^{II}(dhbip)(H_2dcbpy)Cl]Cl$	344 (2.9), 358 (3.5)	310 (3.9)	518 (1.2)	—	—
8 $[Ru^{II}(dhbip)(Hdcbpy)(NCS)]$	347 (3.0), 363 (3.9)	308 (4.2)	500 (1.3)	800	60

[a] Molar absorption coefficients (±5%) in parentheses. [b] Measured in water at pH 1.0. [c] Measured in water at pH 12.

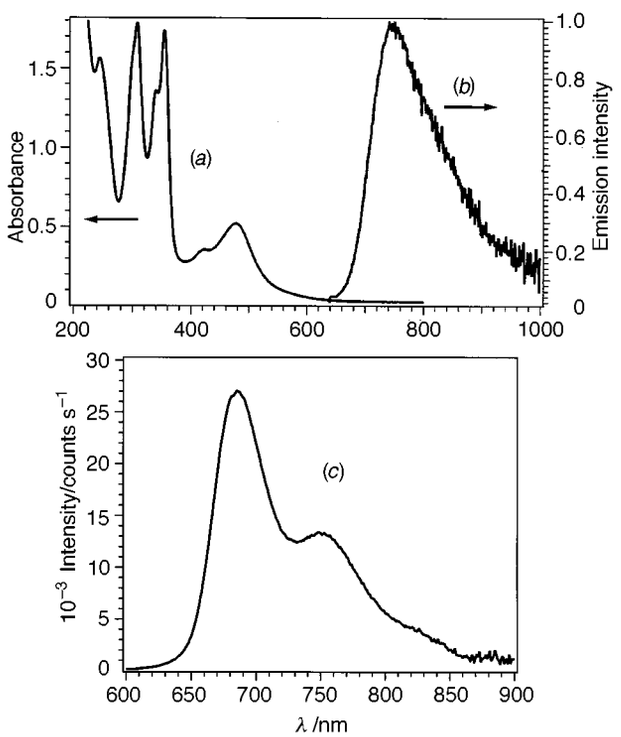

Fig. 1 Absorption (*a*) and emission (*b*) spectra of complex **6**, concentration 4×10^{-4} M in ethanolic solutions at room temperature; (*c*) 77 K emission spectrum in an ethanol–methanol (4 : 1) glass

Absorption spectra

The absorption and luminescence spectral properties of complexes **1**–**10** are summarized in Table 2. The absorption maxima are listed for the intense lowest-energy MLCT bands in ethanol, although the spectra possess additional absorption features at lower and higher energies. Fig. 1 shows typical absorption and emission spectra of complex **6** in ethanol solution. All the ruthenium(II) complexes presented show intense UV bands at 362, 346, 308 and 246 nm. The bands at 362 and 346 nm are assigned to the intraligand π–π* transition of 2,6-bis(1-methylbenzimidazol-2-yl)pyridine. Those at 308 and 244 nm are due to π–π* transition of the dcbpy ligand. Upon acidification, the band at 308 nm shifts to 314 nm due to protonation of the carboxylate groups, while those at 362 and 342 nm remain at acidic and basic pH.

The interesting feature of these complexes is a broad MLCT absorption band in the visible region with a maximum at 500 nm, where the molar absorption coefficient is in the range from ≈9000 to 14 000 M^{-1} cm^{-1}. The MLCT bands of these complexes are broad and red shifted, compared to those of $[Ru^{II}(dcbpy)_3]^{4-}$. This observed red shift could result from (*a*) an increase in the energy of the t_{2g} metal orbital (for example in complexes **3** and **5**), (*b*) a decrease in the π* level of the ligand (complex **9**), or (*c*) the combined effects of both (*a*) and (*b*) (complex **4**), compared to $[Ru^{II}(dcbpy)_3]^{4-}$.

The low-energy MLCT band of complex **10** red shifts from 500 to 528 nm upon going from neutral to basic solution at pH 12. The red shift is assigned to deprotonation of the aqua ligand. The OH^- ligand is a strong donor which causes destabilization of metal t_{2g} orbitals and brings them closer to the ligand π* orbitals. Wrighton and co-workers[17] found a similar red shift from 450 to 500 nm caused by deprotonation of the two hydroxy groups of 4,7-dihydroxy-1,10-phenanthroline (dhphen) in a complex of the type $[RuL_2(dhphen)]$.

Upon acidification, the low-energy MLCT band of complex **10** also shifts from 500 to 514 nm. The red shift of 14 nm is due to protonation of the carboxylate groups, which causes a decrease in the energy of the π* orbital of the dcbpy ligand.[18,19]‡ The energy of the MLCT transition in these complexes decreases in the following order **6** > **7** > **10** > **3**, which is consistent with the decrease in the π-acceptor strength of the ancillary ligand, *i.e.* CN, NCS, H_2O, Cl. The 86 nm red

‡ One of the referees pointed out that protonation of the carboxy groups lowers the π* levels as well as the d_π levels.

Table 3 Absorption and luminescence properties of [Ru^{II}(dhbip)(Hdcbpy)(NCS)] in various solvents

Solvent	Absorption, λ_{max}/nm			Emission λ_{max}/ at 298 K
	π–π* dhbip	π–π* dcbpy	$d_{\pi-\pi^*}$	
EtOH	347, 363	308	500	800
dmso	349, 364	309	518	798
$CHCl_3$	353, 370	310	510	818
CH_2Cl_2	351, 368	312	511	821
MeOH	345, 361	307	502	810
Water	353, 365	309	499	777

shift of the absorption maxima, for complex **9** compared to **7**, is due to the low π* orbital of the biquinoline ligand. The electrochemical data, discussed later (Table 7), of these two complexes are consistent with the above interpretation.

Charge-transfer transitions are also solvent sensitive,[20] and the positions of the lowest-energy absorption maxima for complexes **3**–**10** show solvatochromism. The MLCT band position of complex **8** is listed in Table 3 for various solvents of differing polarity. The 20 nm red shift on going from water to dimethyl sulfoxide (dmso) is due to the lower relative permittivity of the latter. An added advantage of complex **8** is that it is soluble in most of the organic solvents and insoluble in water. This type of hydrophobic sensitizer is particularly useful to prevent water-induced desorption from the semiconductor surface.

Emission spectra

The emission spectra of complexes **7** and **6**, in aqueous solution at pH 11, consist of a single band with a maximum at 800 and 750 nm, respectively (Table 2). The excitation of these complexes at different wavelengths within the manifold of the MLCT band gave the same emission maxima. This phenomenon shows that exciting the complex between 400 and 600 nm leads to population of the same luminescent state. The emission quantum yields for these complexes are significantly lower at neutral and acidic pH, when compared to that of a basic solution. The low quantum yields at acidic pH could be due to proton-induced quenching of the emission.[21] Chloro complexes **3**–**5** are non-emissive at room temperature whereas **10** is weakly emissive.

The emission and absorption spectral properties of complex **8** in various solvents are presented in Table 3. The emission maximum of this complex shows a 25 nm red shift upon going from a high to a low relative permittivity solvent. Complex **9** in dmf gave the most red-shifted absorption (580 nm) and emission spectrum reported here (900 nm), consistent with the reported biq complexes of ruthenium.[22] The emission spectra of complexes **7** and **6** at 77 K [Fig. 2(*c*)] were measured in ethanol–methanol (4 : 1) glasses. They show structured emission with a vibrational progression of 1210 cm^{-1}. The luminescence intensity decreases with increasing temperature.

Determination of pK_a. The pK_a values of complex **10** were determined by spectrophotometric titration. An aqueous stock solution (5×10^{-5} M) was prepared, in water (100 cm^3) containing 0.1 M LiCl, and the initial pH was adjusted to 12 by adding 0.1 M NaOH solution. The UV/VIS spectrum of each solution was obtained after adding acid and allowing the solution to equilibrate for 5 min. Complex **10** in water at pH 12 shows a strong visible band at 528 nm. The other high-energy bands at 358, 343 and 309 nm are due to intraligand transitions of the dmbip and dcbpy, respectively. An unresolved shoulder is present at 406 nm; this could be due to a metal-centered (d–d) charge-transfer transition. The pK_a values of the ground state can be determined from the relationship between the change in optical density with pH at a given wavelength.

Fig. 2(*a*) shows a titration curve obtained by plotting the

Table 4 pK_a Values of the co-ordinated water molecule and dcbpy ligand

Complex	L	L′	pK_a	
			H_2O	CO_2H
[RuL(L′)(H_2O)]	bpz	terpy	8.8[a]	
[RuL(L′)(H_2O)]	bpy	terpy	9.7[b]	
[RuL(L′)(H_2O)]	phen	terpy	9.6[c]	
[RuL(L′)(H_2O)]	tmen	terpy	10.2[c]	
[RuL(L′)(H_2O)]	dcbpy	dmbip	11.4[d]	2.2, 1.4
[RuL(L′)(CN)]	dcbpy	dmbip	—	2.5, —

[a] Ref. 26. [b] Ref. 24. [c] Ref. 25. [d] This work.

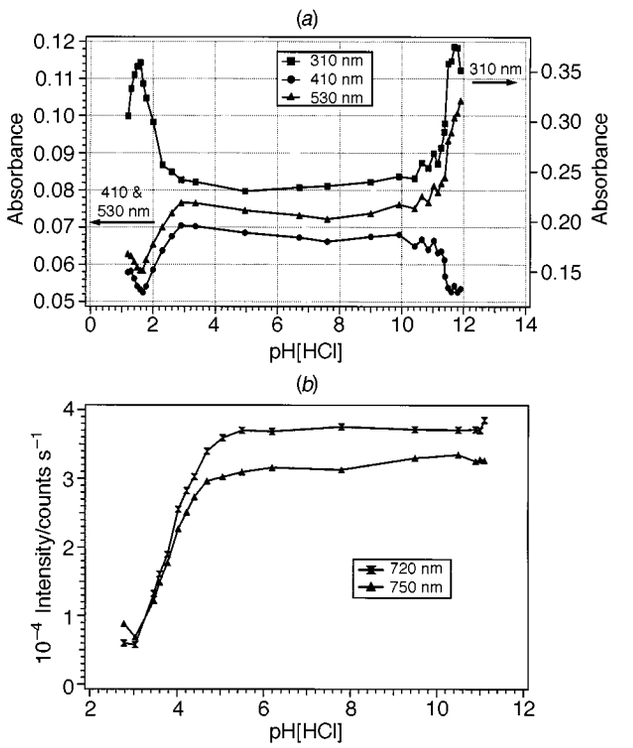

Fig. 2 (*a*) Absorbances as a function of pH for complex **10** containing 0.1 M NaCl at 310, 410 and 530 nm; (*b*) pH dependence of emission intensities of complex **6** in water containing 0.1 M NaCl, excited at 490 nm, emission intensities at 720 and 750 nm

absorbance change at 530, 410 and 310 nm *vs.* pH. The inflection point at pH 11.4 is due to the proton dissociation of the aqua ligand on to the ruthenium center. Meyer and coworkers[23] have reported the pK_a of aqua ligands in ruthenium(II) complexes as 9.7 and 10.8 in the cases of terpyridine and tris(pyrazol-1-yl)methane as spectator ligands, respectively. The striking difference in the pK_a of the aqua ligand in complex **10** to that of the terpyridine analog can be rationalized based on the donor/acceptor properties of dmbip and terpyridine, respectively. The pK_a values of the co-ordinated water molecules in a series of ruthenium complexes with bidentate bpy,[24] phen, tetramethylethylene-1,2-diamine,[25] bpz (2,2′-bipyrazine)[26] and terpyridine ligands are presented in Table 4. As the σ-donor ability of the bidentate ligand increases the redox potential of the metal decreases. In these complexes, the pK_a value of the water molecule increases with increasing ligand basicity. Our present finding for complex **10** is in accord with the literature. In complex **10** the 28 nm red shift of the MLCT maximum going from neutral to basic solution pH 12 is due to the hydroxo ligand, which acts as a strong σ and π donor causing destabilization of the metal t_{2g} orbital, resulting in a lower-energy MLCT band. The 14 nm red shift on going from neutral to acidic solution is due to the protonation of the carboxy groups on the dcbpy ligand.

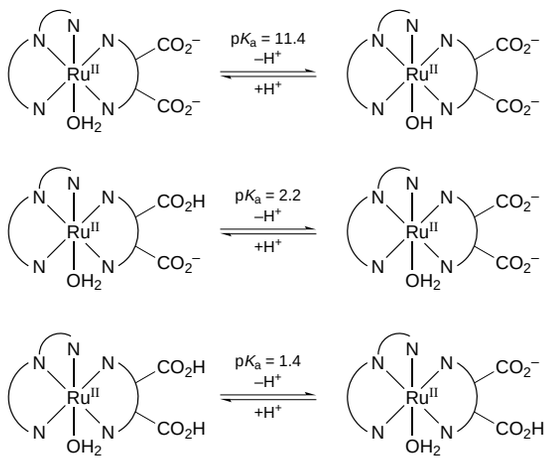

Scheme 1 Ground-state proton-transfer equilibria of [Ru(dmbip)(dcbpy)(H_2O)] **10**

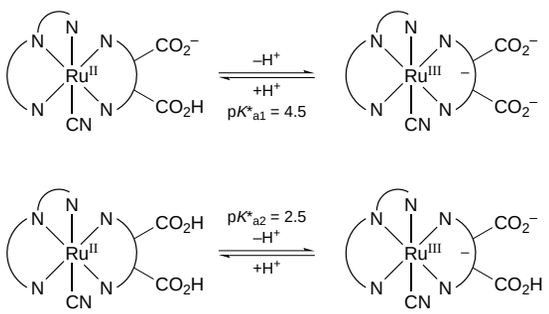

Scheme 2 Excited-state proton-transfer equilibria of [Ru(dmbip)(Hdcbpy)(CN)] **6**

Below pH 3 there are two inflection points [Fig. 2(*a*)] one at pH 2.2 and the other at 1.4, which we assign to the pK_{a1} and pK_{a2} values of the dcbpy ligand. Wrighton and co-workers[27] have investigated the pK_a of [Ru(bpy)$_2$(dcbpy)] and found only one pK_a at 2.7. Lay and Sasse[28] and Shimidzu *et al*.[29] have reinvestigated the acid/base properties of the same complex and found pK_{a1} at 2.7 and pK_{a2} below 0.5. For complex **10**, the fact that we see two inflection points at pH 2.2 and 1.4 suggests that in this complex the dissociation of the carboxy groups is a sequential process (Scheme 1). The pK_{a1} of free dcbpy is 4.2 and the second one is below 2. The difference between the pK_{a1} of free dcbpy and complex **10** is 2 units, which can be considered as a measure of the donor strength of the ligand.

Fig. 2(*b*) shows emission intensity *vs*. pH in ethanol for complex **6**. From spectrofluorimetric titration of complex **6** we were able to estimate the two excited-state pK_a values, one of which is at pK^*_{a1} 4.5 and the second at pK^*_{a2} 2.5 (Scheme 2). The first ground-state pK_a (not shown in the figure) of this complex is at 2.7 and the second one we could not determine because of precipitation of the complex at pH 2.0. The 2 pK_a units difference in the ground and excited state of this complex suggests that the ligand electron density is significantly higher in the excited state because of charge-transfer transition from metal to ligand. In a related system [Ru(dcbpy)$_3$]$^{4-}$ we[19] and others[30] found that the excited state pK_a values are more basic than the ground-state ones. In the excited state the electron is located on the dcbpy ligand and this redistribution of charge creates more electron density on the carboxy groups causing them to be more basic.

RR and IR spectra

The complexes containing thiocyanate and cyanide ligands were characterized by RR and IR spectroscopy. The co-ordination mode of thiocyanate depends on the presence of other ligands around the metal center and the nature of the metal. According to Pearson's soft–hard acid–base theory[31] the presence of strong σ-donor ligands stabilizes the metal–sulfur bond through the π-back bonding, where as π-acceptor ligands enhance nitrogen co-ordination because of lack of electron density on the metal. The temperature also may have a significant effect on the formation of linkage isomers.

The IR spectrum of complex **8** shows intense absorbances at 2107 and 801 cm^{-1} due to thiocyanate ν(NC) and ν(CS), respectively. The observed peaks are consistent with NCS co-ordination through N for most of the structurally characterized transition-metal complexes.[32] The IR and ^{13}C NMR data (presented in NMR section) of these complexes suggest that the thiocyanate co-ordination is through the N.

Resonance-Raman spectroscopy has been used previously to characterize the vibrational structure of the excited MLCT state in polypyridyl metal complexes.[33] This technique was particularly useful in mixed-ligand complexes (heteroleptic complexes) of ruthenium to identify the ligand having the lowest unoccupied molecular orbital (LUMO). In the localized model, Raman excitation of the MLCT band indicates the fully reduced ligand. The assertion is that the electron is localized on the ligand which is the more easily reducible. The RR spectra of the ruthenium complexes were obtained when exciting into the high- and low-energy MLCT bands. Table 5 lists Raman fingerprinting for dmbip and dcbpy vibrations. For comparison purposes, RR data for [Ru(dcbpy)$_2$(NCS)$_2$] and [Ru(dmbip)(dmso)Cl$_2$] are included.

Laser-excitation in the MLCT band of complex **8** at 468 nm yielded detailed resonance-Raman spectra with bands characteristic of both the dhbip and dcbpy ligand [Fig. 3(*a*)]. As the excitation source moved to the red at 520.8 nm enhancement of the modes (relative intensities of the peaks) corresponding to the dcbpy ligand was observed [Fig. 3(*b*)]. The observed bands were assigned by comparing the frequencies of the mixed-ligand complexes and to those of corresponding homoleptic complexes. The Raman spectra of complex **9** obtained by excitation at 520.83 nm gave vibrational modes due to the dcbiq ligand at 1591, 1532, 1458 and 1356 cm^{-1}. The conclusions drawn based on RR spectra were consistent with the previous studies of dcbpy and dcbiq complexes.[34]

The RR spectra obtained by exciting into the MLCT band generally have an underlying signal due to the luminescence of the complex. In order to have a better signal-to-noise ratio in the RR spectra we added freshly prepared silver sol to the measuring solution. The presence of silver sol effectively quenches the luminescence and enhances the RR spectra by surface interactions which is known as the surface-enhanced resonance-Raman scattering (SERRS) effect.[35]

For complexes **7**–**9** the weak band at 2107 cm^{-1} and sharp and intense band at 801 cm^{-1} are due to thiocyanate ν(NC) and ν(CS) stretching vibrations, respectively. The 801 cm^{-1} [ν(CS)] band position is in the range where most *N*-bonded thiocyanate metal complexes are observed. Complex **6** shows a broad and strong band at 2040 cm^{-1}, which is assigned to the ν(CN) stretching mode. Likewise, the vibrational frequencies at 354 and 488 (complex **10**), 387 and 454 (**7**), 387 and 453 (**6**) and 387 and 454 cm^{-1} (**8**) were assigned as ν(M–N) metal–nitrogen vibrational modes.

NMR spectroscopy

The ^{1}H proton NMR spectral data for these complexes are presented in Table 6. Scheme 3 shows the notation for the aromatic protons. The primes refer to the protons of the pyridine ring *trans* to NCS. In these complexes the two pyridine rings of the dcbpy ligand are non-equivalent, hence they show six resonances corresponding to six protons. Based on the integration, position and splitting pattern of the observed peaks, one can distinguish dcbpy resonances from those of dmbip. The co-ordination-induced chemical shift (CIS) ($\delta_{complex} - \delta_{ligand}$) for

Table 5 Resonance-Raman spectroscopic data (cm^{-1}) for ruthenium complexes

Complex	λ_{ex}/nm	4,4′-Dicarboxy-2,2′-bipyridine						2,6-Bis(1-methylbenzimidazol-2-yl)pyridine[a]					
10	520.83	1614	1537	1475	1385	1257	1030		1436	1297	1238		
	476	1606	1532	1469	1373	1252	1036	1445	1432	1293	1231	1019	936
7	520.83	1608	1535	1469	1370	1249	1035	1444	1428	1292	1229	1016	936
	468	1608	1536	1472	1370	1254	1040	1445	1423	1292	1233	1019	937
6	520.83	1608	1536	1471	1375	1268	1024	1564	1511	1291	1234	1024	—
	476.24	1609	1537	1472	1375	1269	1024	1565	1511	1292	1232	1024	997
8	520	1608	1539	1469	1370	1261	1030	1506	1439	1302	1217	1016	941
	468	1608	1539	1468	1365	1260	1034	1506	1440	1301	1216	1015	940
11[b]	468	1612	1539	1477	1295	1269	1045	—	—	—	—	—	—
12[c]	406	—	—	—	—	—	—	1510	1446	1304	1126	1008	

[a] In the case of complex **8**, 2,6-bis(1-hexylbenzimidazol-2-yl)pyridine. [b] $[Ru(dcbpy)_2(NCS)_2]$. [c] $[Ru(dmbip)(dmso)Cl_2]$.

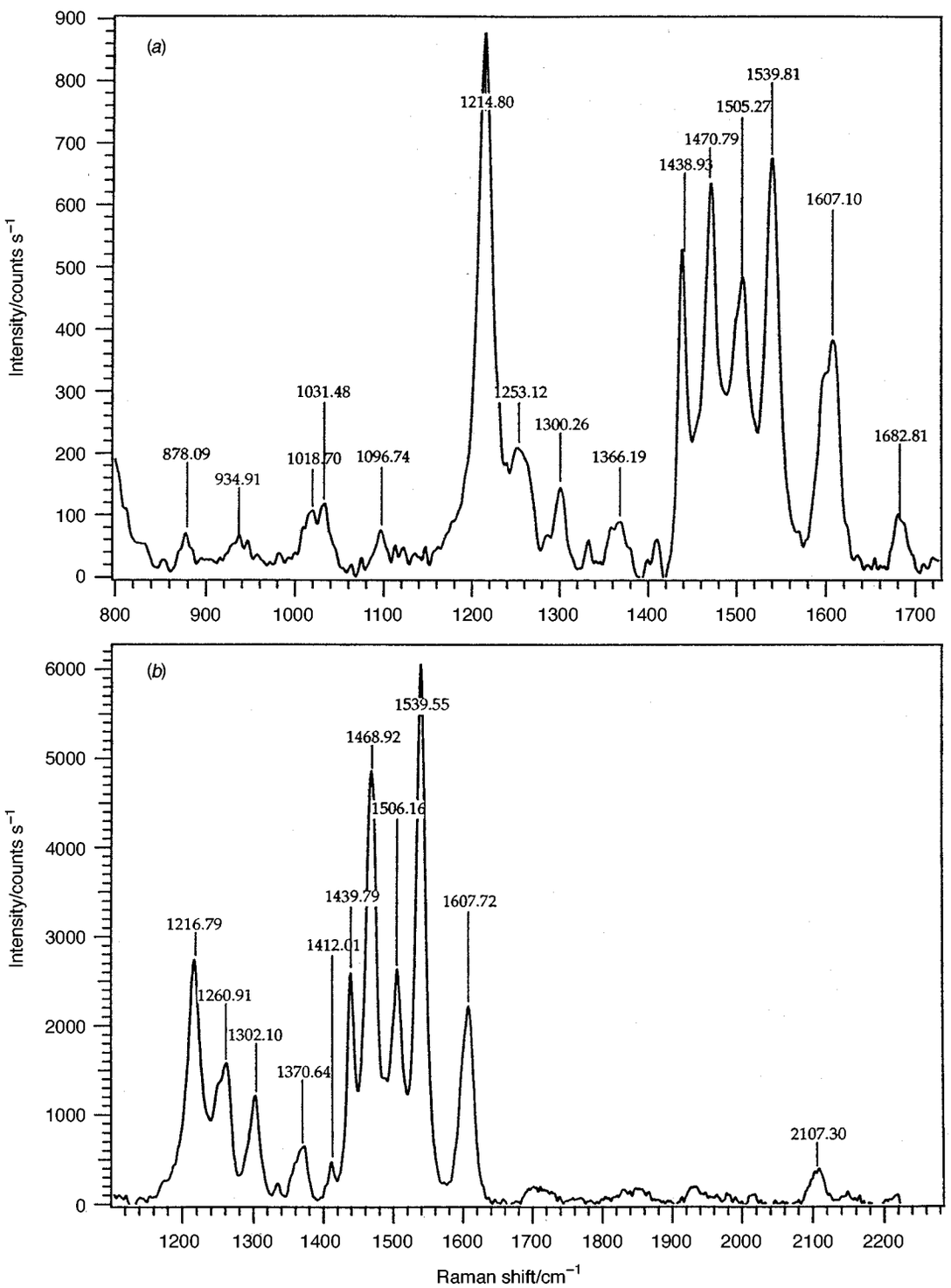

Fig. 3 Resonance-Raman spectra of the mixed-ligand complex **8** in aqueous solution at (*a*) 468 nm excitation, (*b*) at 520.83 nm excitation

Table 6 Proton NMR spectral data (δ) for ruthenium complexes measured in CD_3OD

	4,4′-Dicarboxy-2,2′-bipyridine						2,6-Bis(1-methylbenzimidazol-2-yl)pyridine					
Complex	H(6)	H(6′)	H(3)	H(3′)	H(5)	H(5′)	H(1)	H(2)	H(6)	H(7)	H(8)	H(9)
dcbpy[a]	8.78 (d)		8.4 (d)		7.87 (dd)							
dhbip	—	—	—	—	—	—	8.09 (t)	8.32 (d)	7.9 (d)	7.35 (t)	7.35 (t)	7.5 (d)
[Ru(dmbip)(dmso)Cl_2]	—	—	—	—	—	—	8.18 (t)	8.53 (d)	8.63 (d)	7.6 (t)	7.51 (t)	7.83 (d)
[Ru(dmbip)(dcbpy)-(H_2O)][b]	10.16 (d)	6.92 (m)	9.06 (s)	8.52 (s)	8.49 (dd)	7.32 (m)	8.16 (t)	8.60 (d)	7.32 (m)	7.15 (t)	6.92 (m)	6.17 (d)
[Ru(dmbip)(Hdcbpy)-(NCS)]	10.28 (d)	7.6 (d)	9.22 (s)	8.70 (s)	8.49 (dd)	7.25 (dd)	8.11 (t)	8.64 (d)	7.64 (d)	7.35 (t)	7.02 (t)	6.25 (d)
[Ru(dmbip)(Hdcbpy)-(CN)]	10.54 (d)	7.32 (d)	9.19 (s)	8.82 (s)	8.38 (dd)	7.45 (dd)	8.3 (t)	8.7 (d)	7.66 (d)	7.36 (t)	7.06 (t)	6.23 (d)
[Ru(dhbip)(Hdcbpy)Cl]	11.3 (d)	7.38 (d)	9.99 (s)	8.71 (s)	8.4 (dd)	7.39 (dd)	8.23 (t)	8.71 (d)	7.67 (d)	7.35 (t)	7.07 (t)	6.3 (d)
[Ru(dhbip)(Hdcbpy)-(NCS)]	10.19 (d)	7.66 (d)	9.23 (s)	8.77 (s)	8.5 (dd)	7.34 (dd)	8.32 (t)	8.57 (d)	7.68 (d)	7.37 (t)	7.08 (t)	6.2 (d)

[a] Measured in D_2O. [b] In alkaline CD_3OD.

Table 7 Ground- and excited-state redox potentials of ruthenium complexes

	$E_{\frac{1}{2}}$/V *vs.* SCE		*E**/V		
Complex[a]	Oxidation	Reduction	Oxidation	Reduction	IPCE[b] (%)
[Ru(dmbip)(dcbpy)(H_2O)]	0.71	−1.35	−0.85	0.2	85
[Ru(dmbip)(Hdcbpy)(NCS)]	0.8	−1.3	−0.75	0.25	75
[Ru(dmbip)(dcbpy)(CN)][c]	0.92	−1.35, −1.51	−0.73	0.3	60
[Ru(dmbip)(Hdcbiq)Cl]	0.83	−0.91, −1.17			—
[Ru(dmbip)(Hdcbiq)(NCS)][d]	1.15	−0.85, −1.03	−0.23	0.53	⩽10
[Ru(dhbip)(H_2dcbpy)Cl]Cl[e]	0.67	−1.35, −1.48			—
[Ru(dhbip)(Hdcbpy)(NCS)][e]	0.81	−1.34, −1.48	−0.74	0.22	70

[a] Measured in EtOH with 0.1 M tetrabutylammonium tetrafluoroborate. [b] Measured at absolute maximum with the thin-layer cell containing an electrolyte of 0.03 M I_2 and 0.3 M LiI in ethanol. [c] In dmso. [d] In dmf, irreversible. [e] In CH_2Cl_2, quasi-reversible.

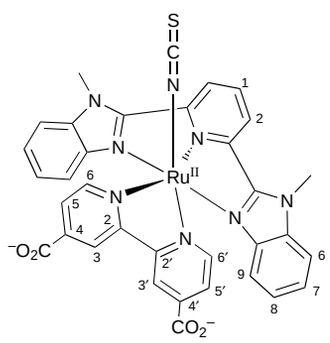

Scheme 3

equatorial pyridine is more positive than for the axial pyridine, which is *trans* to NCS. Positive values refer to downfield shifts.

It is interesting that the lowest-field dcbpy doublet H(6) is found to be the most sensitive indicator. Its position can vary over a range of about 1.1 ppm in going from a chloro to a thiocyanato complex, whereas the other peaks vary over 0.2 ppm. For a chloro complex the H(6) proton is shifted more downfield compared to H_2O, CN^- and NCS^- as ligands. The peaks in the aliphatic region at δ 4.5 are due to the alkyl protons on the imidazole nitrogen.

Proton-decoupled ^{13}C NMR spectra of these complexes were measured in either D_2O or $CDCl_3$. The spectra of ruthenium complexes containing thiocyanate are useful to identify the mode of NCS co-ordination. It has been reported that sulfur co-ordination of NCS to transition metals shields the carbon atom much more than does nitrogen co-ordination.[36] Based on our systematic studies of ruthenium complexes containing thiocyanate,[37] we assign the resonance peak at δ 135 to *N*-bonded thiocyanate carbon.

Ground- and excited-state redox potentials

The ground- and excited-state redox potentials of these complexes are collected in Table 7. The cyclic voltammogram of complex **5** measured in dichloromethane solvent shows one reversible wave at 0.67 V *vs.* saturated calomel electrode (SCE), with 90 mV separation between the anodic and cathodic peaks. In reduction there are two quasi-reversible waves at −1.35 and −1.48 V *vs.* SCE. For bis dmbip complexes of ruthenium the first reduction potential was observed at −1.4 V *vs.* SCE. Hence we assign the two reduction waves of complex **5** as due to dcbpy and dhbip respectively. Substitution of the chloro ligand by aqua (complex **10**), NCS (**7**) and CN (**6**) results in a steady increase in the potential of the $Ru^{III/II}$ couple from 0.67 to 0.92 V *vs.* SCE, illustrating the fine tuning of the redox potentials by selecting appropriate ligands. There have been few studies of tuning of the energy of the Ru (t_{2g}) level.[38] Our results are in agreement with the literature.

The increase in oxidation potential from chloro to cyanide ligand in these complexes is consistent with the π-acceptor nature of cyanide and σ-donor nature of chloride. It is interesting to compare the first reduction potential of complex **9** which is anodically shifted by 450 mV compared to that of **7**. This difference could be due to the greater π-acceptor nature of dcbiq. Owing to this, in the excited state complex **8** is less reducing than are the dcbpy analogues.

Photovoltaic performance

The performance of the ruthenium complexes as sensitizers on nanocrystalline TiO_2 electrodes has been studied. The preparation of the nanostructured TiO_2 films and experimental details for the measurements were given earlier.[7,8] All the dye solutions were prepared in distilled ethanol and typical concentrations were in the $(1–3) \times 10^{-4}$ M range. The TiO_2 electrodes were coated by dipping in the dye solutions for 3–5 h. Table 7 presents the IPCE (incident photon to current efficiency) values of these dyes calculated by using equation (1). All the values were

$$\text{IPCE} = \frac{1.24 \times 10^3 \times \text{photocurrent density (mA cm}^{-2})}{\text{Wavelength (nm)} \times \text{photon flux (W m}^{-2})} \quad (1)$$

measured on thin-layer nanocrystalline TiO_2 electrodes with $I–I_3^-$ as the redox electrolyte in ethanol solvent. The values increase with decreasing excited-state oxidation potential. The efficiencies for this series of complexes increase in the order **3** < **6** < **7** ≈ **10**. Complex **9** under these conditions shows less than 10% photon to electron injection efficiency.

The apparent difference between dcbpy and dcbiq complexes could be due to a combination of many factors. The excited-state oxidation potential of the dcbiq complex is less negative compared to the dcbpy complex, hence the excited state is not as energetically favorable to enable transfer of an electron into the conduction band of the TiO_2 semiconductor. The excited-state lifetime of complex **9** could be too short for the process of electron injection into the conduction band of the TiO_2 electrode to be efficient. However, the aqua complex **10** gives injection efficiencies close to 80%,[7] and it has a short excited-state lifetime (<5 ns). Also, it has been reported that the interfacial electron-transfer processes on TiO_2 electrodes are in the femtosecond domain.[39] Based on the above considerations, it appears that the excited-state oxidation potential plays a more crucial role than the lifetime of the sensitizer molecule in the interfacial electron-transfer processes. Further evidence for this hypothesis is obtained when the conduction band of the TiO_2 electrode is lowered, by the addition of an acid (electrolyte pH ≈ 1), where complex **9** shows practically quantitative photon to electron injection efficiency.

Conclusion

In this paper we have demonstrated tuning of the ground and excited-state redox potentials by carefully selecting the donor ligands like Cl^-, H_2O, CN^-, NCS^-. The MLCT transitions have been tuned from 500 to 580 nm by changing the acceptor ligand dcbpy to dcbiq. By substituting long aliphatic chains on the 2,6-bis(benzimidazol-2-yl)pyridine the hydrophobicity was increased; this type of sensitizer is particularly useful to prevent water-induced desorption from the semiconductor surface. An additional feature in complex **8** is an increase in its solubility in most of the organic solvents.

Spectrophotometric titration of the ruthenium complex containing an aqua ligand reveals the pK_a at 11.4. Quantitative analysis of the spectral changes below pH 4 yields two pK_a values for the ground state. The excited-state pK_a values are 2 units more basic than the ground-state ones. Using resonance-Raman spectroscopy we have identified the lowest-energy MLCT transitions, which are localized on acceptor ligands like dcbpy and dcbiq. Furthermore, the cyclic voltammograms of these complexes suggest that the reductions are localized on the dcbpy or dcbiq ligands. The excited-state oxidation potentials were calculated and compared with the efficiencies of the interfacial electron injection on TiO_2 semiconductor electrodes. The excited-state oxidation potential plays a more crucial role in the electron-transfer process than the excited-state lifetime of the sensitizer.

Acknowledgements

This work was supported by a grant from the Swiss Federal Institute for Energy (OFEN).

References

1 G. J. Ferraudi, *Elements of Inorganic Photochemistry*, Wiley-Interscience, New York, 1988.
2 D. M. Roundhill, *Photochemistry and Photophysics of Metal Complexes*, Plenum, New York, 1994.
3 A. Juris, V. Balzani, F. Barigelletti, S. Campagna, P. Belser and A. von Zelewsky, *Coord. Chem. Rev.*, 1988, **84**, 85.
4 K. A. Opperman, S. L. Mecklenburg and T. J. Meyer, *Inorg. Chem.*, 1994, **33**, 5295.
5 F. Scandola, M. T. Inddelli and C. A. Bignozzi, *Top. Curr. Chem.*, 1990, **158**, 73; F. Scandola, C. A. Bignozzi and M. T. Inddelli, *Photosensitization and Photocatalysis Using Inorganic and Organometallic Compounds*, Kluwer, Dordrecht, 1993, pp. 161–216.
6 G. J. Ashwell, *Molecular Electronics*, RSP Ltd., Taunton, 1991.
7 P. Liska, N. Vlachopoulos, Md. K. Nazeeruddin, P. Compte and M. Grätzel, *J. Am. Chem. Soc.*, 1988, **110**, 3686.
8 Md. K. Nazeeruddin, A. Kay, I. Rodicio, R. Humphry-Baker, E. Müller, N. Vlachopoulos and M. Grätzel, *J. Am. Chem. Soc.*, 1993, **115**, 6382; R. Argazzi, C. A. Bignozzi, T. A. Heimer, F. N. Castellano and G. J. Meyer, *Inorg. Chem.*, 1994, **33**, 5741; K. Murakoshi, G. Kano, Y. Wada, S. Yanagida, H. Miyazaki, M. Matsumoto and S. Murasawa, *J. Electroanal. Chem.*, *Interfacial Electrochem.*, 1995, **396**, 27.
9 K. Kalyanasundaram, M. Grätzel and Md. K. Nazeeruddin, *J. Chem. Soc.*, *Dalton Trans.*, 1991, 343; S. Campagna, G. Denti, L. Sabatino, S. Serroni, M. Ciano and V. Balzani, *J. Chem. Soc.*, *Chem. Commun.*, 1989, 1500.
10 K. Kalyanasundaram and Md. K. Nazeeruddin, *Chem. Phys. Lett.*, 1992, **193**, 292.
11 P. A. Anderson, G. F. Strouse, J. A. Treadway, F. R. Keene and T. J. Meyer, *Inorg. Chem.*, 1994, **33**, 3863.
12 M. Maestri, N. Armaroli, V. Balzani, E. C. Constable and A. M. W. Cargill Thompson, *Inorg. Chem.*, 1995, **34**, 2579.
13 F. Bargelletti, L. Flamigni, V. Balzani, J.-P. Collin, J.-P. Sauvage, A. Sour, E. C. Constable and A. M. W. Cargill Thompson, *J. Chem. Soc.*, *Chem. Commun.*, 1993, 942.
14 C. G. Bochet, C. Piguet and A. F. Williams, *Helv. Chim. Acta*, 1993, **76**, 372.
15 C. Piguet, B. Bocquet, E. Müller and A. F. Williams, *Helv. Chim. Acta*, 1989, **72**, 323.
16 (*a*) B. A. Moyer and T. J. Meyer, *J. Am. Chem. Soc.*, 1978, **100**, 3601; (*b*) O. Kohle, S. Ruile and M. Grätzel, *Inorg. Chem.*, 1996, **35**, 4779.
17 P. J. Giordano, C. R. Bock and M. S. Wrighton, *J. Am. Chem. Soc.*, 1978, **100**, 6960.
18 A. M. W. Cargill Thompson, M. C. C. Smailes, J. C. Jeffery and M. D. Ward, *J. Chem. Soc.*, *Dalton Trans.*, 1997, 737.
19 M. K. Nazeeruddin and K. Kalyanasundaram, *Inorg. Chem.*, 1989, **28**, 4251.
20 J. C. Curtis, B. P. Sullivan and T. J. Meyer, *Inorg. Chem.*, 1983, **22**, 224.
21 K. Kalyanasundaram and M. K. Nazeeruddin, *Inorg. Chim. Acta*, 1990, **171**, 213.
22 G. Denti, S. Campagna, L. Sabatino, S. Serroni, M. Ciano and V. Balzani, *Inorg. Chem.*, 1990, **29**, 4750.
23 K. J. Takeuchi, M. S. Thomson, D. W. Pipes and T. J. Meyer, *Inorg. Chem.*, 1984, **23**, 1845.
24 A. Llobet, P. Doppelt and T. J. Meyer, *Inorg. Chem.*, 1988, **27**, 514.
25 N. Gupta, N. Grover, G. A. Neyahart, P. Sing and H. H. Throrp, *Inorg. Chem.*, 1993, **32**, 310.
26 A. Gerli, J. Reedijk, M. T. Lakin and A. L. Spek, *Inorg. Chem.*, 1995, **34**, 1836.
27 P. J. Giordano, C. R. Bock and M. S. Wrighton, *J. Am. Chem. Soc.*, 1978, **100**, 1170.
28 P. A. Lay and W. H. S. Sasse, *Inorg. Chem.*, 1984, **23**, 4123.
29 T. Shimidzu, T. Iyoda and K. Izaki, *J. Phys. Chem.*, 1985, **89**, 642.
30 P. J. Giordano, C. R. Bock, M. S. Wrighton, L. V. Interrante and R. F. X. Williams, *J. Am. Chem. Soc.*, 1977, **99**, 3187.
31 R. G. Pearson, *J. Am. Chem. Soc.*, 1963, **85**, 3533.
32 S. Wajda and K. Rachlewicz, *Inorg. Chim. Acta*, 1978, **31**, 35.
33 Y. Fuchs, S. Lofters, T. Dieter, W. Shi, R. Morgan, T. C. Strekas, H. Gafney and A. D. Baker, *J. Am. Chem. Soc.*, 1987, **109**, 2691.
34 M. K. Nazeeruddin, M. Grätzel, K. Kalyanasundaram, R. B. Girling and R. E. Hester, *J. Chem. Soc.*, *Dalton Trans.*, 1993, 323.
35 T. J. Dines and R. D. Peacock, *J. Chem. Soc.*, *Faraday Trans. 1*, 1988, 3445.
36 J. A. Kargol, R. W. Crecely and J. L. Burmeister, *Inorg. Chem.*, 1979, **18**, 2532.
37 V. Shklover, M. K. Nazeeruddin, S. M. Zakeeruddin, C. Barbe, A. Kay, T. Haibach, W. Steurer, R. Hermann, H.-U. Nissen and M. Grätzel, *Chem. Mater.*, 1997, **9**, 430.
38 J. V. Caspar and T. J. Meyer, *Inorg. Chem.*, 1983, **23**, 2444.
39 F. Willig, R. Eichberger, N. S. Sundaresan and B. A. Parkinson, *J. Am. Chem. Soc.*, 1990, **112**, 2702.

Received 17*th June* 1997; *Paper* 7/04242F